

## Formation of a rotating hole from a close limit head-on collision

William Kavan

Department of Physics, University of Utah, Salt Lake City, UT 84112  
and Institut für Astronomie und Astrophysik, Universität Tübingen, D-72076 Tübingen, Germany

Richard H. Price

Department of Physics, University of Utah, Salt Lake City, UT 84112

Realistic black hole collisions result in a rapidly rotating Kerr hole, but simulations to date have focused on nonrotating holes. Using a new solution of the Einstein initial value equations we present here waveforms and radiation for an axisymmetric Kerr-hole-forming collision starting from small initial separation (the "close limit" approximation) of two identical rotating holes. Several new features are present in the results: (i) In the limit of small separation, the waveform is linear (not quadratic) in the separation. (ii) The waveforms show damped oscillations mixing quasinormal ringing of different multipoles.

04.25.Dm, 95.30.Sf, 97.60.Lf

The study of black hole collisions with numerical relativity [1] will give unprecedented insights into the nonlinear workings of relativistic gravitation in strong field situations and is expected to provide important information about the waves that may be observable with the gravitational wave detectors currently under construction [2]. In the difficult task of developing collision codes it has been found useful to compare numerical relativity results with those of "close limit" calculations [3]. In these calculations the black holes are taken to start at a small separation, and the initial separation is used as a perturbation parameter. The collisions of primary interest are those with high angular momentum that end in the formation of a rapidly rotating Kerr black hole. This is based on the expectation that such collisions are the endpoint of binary inspiral and that collisions with high angular momentum will produce much more gravitational radiation than collisions leading to a nonrotating hole. But the close limit method has so far been applied only to collisions resulting in a nonrotating, or slowly rotating hole. There are two reasons for this.

The first reason is a technical one. The starting point of the dynamics of a collapse is a spatial metric  $^{(3)}g_{ij}$  and an extrinsic curvature  $K_{ij}$  that solve Einstein's initial value equations. For the close limit perturbation method to be used for rotating holes, these initial value solutions must be a perturbation of a Kerr spacetime. But the prevalent method for specifying initial data, the conformally flat prescription of Bowen and York [4], is incompatible with the Kerr solution, for which the standard slicing, at least, is not conformally flat. A family of close limit perturbations of Kerr initial data, then, could not

be given in the Bowen-York formalism.

This technical difficulty is no longer a barrier. New axisymmetric initial data solutions representing two rotating holes have recently been given by Baker and Puzio [5], and by us [6]. In both types of solutions close limit sequences of initial data can be constructed for holes starting a head-on axisymmetric collision. More specifically, a sequence can be constructed for different initial separations, with the close limit of the sequence being the Kerr spatial geometry and extrinsic curvature outside a Kerr horizon. We have chosen to start with the close limit initial data set of Ref. [6] based on the Brill-Brandt-Seidel [7] form of the 3-metric and of the nonvanishing components of extrinsic curvature,

$$ds^2 = -e^{2q} dr^2 + r^2 d\theta^2 + r^2 \sin^2 \theta d\phi^2; \quad (1)$$

$$K_r = r^{-2} \mathcal{H}_E \sin^2 \theta; \quad K_\theta = r^{-1} \mathcal{H}_F \sin \theta; \quad (2)$$

in which  $q; \mathcal{H}_E; \mathcal{H}_F$  are functions of  $r; \theta$ . For the appropriate choices  $\mathcal{K}; \mathcal{K}_K; \mathcal{H}_{EK}; \mathcal{H}_{FK}$ , these become the metric and extrinsic curvature for a slice of Kerr spacetime at constant Boyer-Lindquist [8] time. In this case the coordinate of (1) and (2) is the same as the Boyer-Lindquist  $\rho$ , and the Boyer-Lindquist radial coordinate  $r$  is a rescaling of  $\rho$ , depending on the Kerr parameters  $M; a$ , as given in Ref. [6].

In our approach to an initial value solution we take  $q, \mathcal{H}_E, \mathcal{H}_F$  to have precisely their Kerr forms  $\mathcal{K}, \mathcal{H}_{EK}, \mathcal{H}_{FK}$ . It turns out that this guarantees that all of the initial value equations are satisfied except one, the Hamiltonian constraint, an elliptic equation for  $\mathcal{K}$ . Boundary conditions for this equation must be chosen in order to complete the specification of a solution. One condition is asymptotic flatness. If for the other condition we choose to have  $\mathcal{K} = r$  as  $r \rightarrow 0$ , then we find the Kerr solution  $\mathcal{K}$  if  $\mathcal{H}_{sing}$  is chosen appropriately. (Otherwise we find a distorted Kerr hole.) To arrive at an initial value solution representing two initial holes, we choose two point-like singularities on the  $z$  axis in the  $r; \theta$  plane, and we place them at  $z = \pm z_0$  (that is, at  $r = z_0; \theta = 0$ ). The parameter  $z_0$ , then, describes the initial separation between the two holes. It is shown in Ref. [6] that the  $z_0 \rightarrow 0$  limit of the initial solution is the Kerr geometry, outside the Kerr horizon, with mass  $M$  and spin parameter  $a$  (the parameters chosen

for the functions  $q_K; \dot{\Phi}_{EK}; \dot{\Phi}_{FK}$ ). In the limit of small  $z_0$ , the 3-geometry and extrinsic curvatures are perturbations away from the Kerr forms. This provides the starting point for evolving perturbations on a Kerr background.

The second reason that close limit calculations have previously been limited to collisions forming a Schwarzschild (nonrotating) hole is that no numerical relativity results were available of collisions leading to Kerr formation. This can, of course, be viewed as an opportunity to provide the only available (though very limited) answers about the nature of collisions to form Kerr holes. But our real motivation in presenting these results is to continue the useful interaction of perturbation studies and numerical relativity. In particular, we hope that these results stimulate work on fully nonlinear evolution of initial data solutions amenable to close limit perturbation methods, and hence to comparisons.

Linearized evolution for perturbations of the Kerr geometry is carried out with the Teukolsky equation [9], rather than the Zerilli [10] or Regge-Weeler [11] equation of Schwarzschild perturbations. The introduction of the Teukolsky equation entails two new elements in a calculation. Since the Kerr background is not spherically symmetric, its perturbations cannot be decomposed into spherical harmonics [12]. The dependence on a polar angle cannot therefore be separated. The linearized numerical evolution must be carried out as a solution of a 2+1 variable  $(r; t)$  linear hyperbolic differential equation, rather than a 1+1 variable  $(r; t)$  equation for each multipole of spherical perturbations. (Since we are discussing the evolution of perturbations of the Kerr spacetime, here and below the coordinates  $r; t$  are the standard, i.e., Boyer-Lindquist [8] coordinates for the Kerr spacetime.) To solve the 2+1 partial differential equation we use an existing and thoroughly verified 2+1 evolution code [13]. Though the computational requirements of this code are much greater than for 1+1 codes, they are handled easily by the RAM and speed of large modern workstations. It should be noted that the essential difficulties of numerical relativity lie in the nonlinear equations of Einstein's theory. None of the worst difficulties affect our linearized version of the evolution equations.

The second new feature to be faced is the way in which initial conditions must be handled. In the Zerilli [10] or Regge-Weeler [11] formalism, evolution is carried out for a "wavefunction" that is defined in terms of metric perturbations. It is relatively straightforward to compute the initial wavefunction and its initial time derivative from an initial value solution for  ${}^{(3)}g_{ij}; K_{ij}$ . In the Teukolsky formalism the quantity that is evolved with a wave equation has a somewhat different character. This quantity originates in the Newman-Penrose [14] formalism that encodes information about curvature into

ve complex fields  $\phi_0; \dots; \phi_4$  that are projections of the Weyl tensor (equivalent to the Riemann curvature tensor

$R$  in vacuum) onto a null tetrad of complex vectors  $\ell; n; m; \bar{m}$ . Of particular importance here, is the projection

$$\phi_4 = R_{n\bar{m}n\bar{m}}; \quad (3)$$

since the Teukolsky formalism evolves the wave function

$$(r - ia \cos \theta)^4 \phi_4; \quad (4)$$

It turns out that  $\phi_4$  (and hence  $\phi$ ) is invariant to first order under first order perturbations of the tetrad, so the specification of initial data amounts to the computation of the initial value of  $R_{n\bar{m}n\bar{m}}$ , and its initial time derivative. The computation of the initial  $\phi$  is carried out using the Gau-Codazzi equations [15] which relate the Riemann curvature to  ${}^{(3)}g_{ij}; K_{ij}$  of the initial value solution. Finding the initial  $\phi_t$  requires that we know the initial time derivative of the Weyl tensor. To find this we substitute the first order vacuum Einstein evolution equations for the 3-metric and the extrinsic curvature into the explicit formula for  $\phi_t$ . Though straightforward in principle, the calculation of the initial  $\phi$  and of  $\phi_t$  from the initial  ${}^{(3)}g_{ij}; K_{ij}$  is very lengthy, and subject to error. To carry out the computation, a Maple script was written to find  $\phi$  from the initial data functions  $q; \dot{\Phi}_E; \dot{\Phi}_F$ . The output of the script was checked against analytic expressions known for  $a = 0$  [16]. For  $a \neq 0$  the result was checked numerically against a very different Maple script, kindly supplied by Gaurav Khanna, in which  $\phi_4$  is computed from the linearized perturbations on a Kerr background [17]. In both comparisons the agreement was well within the expected numerical accuracy.

For values restricted to the region outside the event horizon of the Kerr background, it is useful to introduce the radial variable  $r$  defined [18] in terms of the standard (Boyer-Lindquist) radial variable  $\bar{r}$  by  $dr = d\bar{r} = (\bar{r}^2 + a^2)/(\bar{r}^2 - 2M\bar{r} + a^2)$ . The  $r$  variable agrees with  $\bar{r}$  in the limit of large  $\bar{r}$  and approaches  $\infty$  at the unperturbed horizon  $r_+ = M + \sqrt{M^2 - a^2}$ . Since the value of  $\phi_4$  diverges as  $r^3$  for large  $r$  we introduce  $Q = M^{-3}\phi_4$ .

We have chosen to evolve initial solutions representing holes of equal mass and spin, so that each collision is characterized by the set of parameters  $a; M; z_0$  (where  $M$  and  $a$  are the mass and spin parameters of the final Kerr hole), or by the two dimensionless parameters  $a/M; z_0/M$ . Since  $\phi$  and  $\phi_t$  are complex, there are four functions of  $r$  contained in them. Due to the symmetry of the collision these functions all have symmetry properties with respect to the  $\theta = \pi/2$  equatorial plane. Specifically,  $\text{Re } \phi; \text{Re } \phi_t$  are symmetric with respect to the equatorial plane, while  $\text{Im } \phi; \text{Im } \phi_t$  are antisymmetric. The plot of  $\text{Im } \phi_t Q$  as a function of  $r$ , in Fig. 1, shows the antisymmetry of  $\text{Im } \phi_t$  and the vanishing of  $\phi$  at the horizon and at large  $r$ .

In the case  $a = 0$  the conformal factor can be written in analytic form, and it can be shown that in the  $z_0 \rightarrow 0$

limit, the relative deviation from the Schwarzschild geometry is quadratic in  $z_0$ . In the numerically computed solutions for  $\epsilon$ , we find that the relative deviation is generally linear in  $z_0$ . Since this dependence must revert to a quadratic one for  $a \rightarrow 0$ , we infer

$$= F_1(r; \epsilon; a)z_0 + F_2(r; \epsilon; a)z_0^2 + O(z_0^3); \quad (5)$$

where  $F_1$  vanishes, but  $F_2$  does not, as  $a \rightarrow 0$ . A numerical confirmation of this relationship is shown in Fig. 2.

The values of  $\epsilon$  and  $\theta_t$  as described above are next used as Cauchy data for the Teukolsky equation, and the equation is solved numerically to find  $Q(r; \epsilon; t)$ . The real and imaginary parts of  $Q$  correspond to the two distinct linear polarization modes of gravitational waves, and both  $\text{Re}Q$  (solid curve) and  $\text{Im}Q$  (solid curve) are shown in Fig. 3. A semilog plot is used to show most clearly the nature of the oscillations and exponential damping of the waves, after an initial transient. Some features of Fig. 3 have a simple explanation: Although the Kerr background is not spherically symmetric, perturbations at a single frequency can be decomposed into angular functions and one can find the complex quasinormal frequencies for each angular function. For  $\text{Re}Q$  both the damping (slope of the line connecting the peaks) and the oscillation rate (spacing of zeroes) agree to within around 1% with the frequency of the least damped quasinormal frequency [19]  $\omega_2 = (0.388 + i0.086)M$  for the  $\ell = 2$  axisymmetric mode of the  $a/M = 0.6$  hole that is formed in the collision. The explanation of  $\text{Im}Q$  is less simple, but more interesting. It has the appearance of a superposition of ringing at  $\omega_2$  and at  $\omega_3 = (0.618 + i0.088)M$ . For  $t/M > 50$  the dashed curve in fact is indistinguishable from the function

$$4.39 \cdot 10^{-4} \sin(0.388t/M + 0.463) \exp(-0.086t/M) \\ + 8.26 \cdot 10^{-4} \sin(0.618t/M - 1.951) \exp(-0.088t/M);$$

This superposition comes about because the Teukolsky equation mixes real and imaginary parts, through a term involving  $i a \cos \theta$ . The angular dependence of the imaginary part of the initial data gives rise to small  $\text{Im}Q$  evolution characterized by  $\omega_3$ , but during evolution, the oscillations of  $\text{Re}Q$ , at  $\omega_2$  are fed into  $\text{Im}Q$  by the Teukolsky equation. The reverse mixing of  $\text{Im}Q$  into  $\text{Re}Q$  is not of importance because  $\text{Im}Q$  is much smaller than  $\text{Re}Q$ , and mixing is weak.

Figure 4 gives the computed total gravitational wave energy contained in the waveforms, as a function of  $z_0$  for spin parameter values  $a/M = 0; 0.1; 0.2; 0.4$ . The  $a = 0$  problem is equivalent to computations using Schwarzschild perturbation methods, and the results of those methods [20] agree with the  $a = 0$  points in Fig. 4 to better than 1.5%. The figure is somewhat misleading regarding the dependence of radiated energy on angular momentum. The variable  $z_0$  is a formal measure of

separation, not directly connected with a physical separation. A physical separation, for example the proper distance between the intersection of the axis and the apparent horizon, depends on both  $z_0$  and  $a$ . Figure 4, therefore, does not show the influence of rotation on radiation, but it does give results for well specified initial data, results that could be evolved with numerical relativity on supercomputers. We hope that comparisons with such results will be available soon. Another application of these results will be a comparison of predicted waveforms and energies using the slow-rotation approximation (i.e., treating rotation as well as separation as a perturbation), a comparison that will reveal whether slow-rotation methods can be used for fairly rapid rotation. We will provide such a comparison in a more detailed presentation describing the present work.

We thank John Baker, Gaurav Khanna, and Raymond Puzio for helpful suggestions. This work was partially supported by NSF grant PHY-9734871.

- 
- [1] L. S. Finn, in Proceedings of the 14th International Conference on General Relativity and Gravitation, Florence, 1995, edited by M. Francaviglia, G. Longhi, L. Lusanna, E. Sorace (World Scientific, Singapore, 1997), gr-qc/9603004
  - [2] E. E. Flanagan and S. A. Hughes, Phys. Rev. D 57, 4535 (1998).
  - [3] R. H. Price and J. Pullin, Phys. Rev. Lett. 72, 3297 (1994); A. Abraham and R. H. Price, Phys. Rev. D 53, 1963 (1996); J. Pullin, Fields Inst. Commun., 15, 117 (1997); P. Anninos, R. H. Price, J. Pullin, E. Seidel and W.-M. Suen, Phys. Rev. D 52, 4462 (1995); J. Baker, A. Abraham, P. Anninos, S. Brandt, R. Price, J. Pullin, E. Seidel, Phys. Rev. D 55, 829 (1997); O. Nicasio, R. Gleiser, R. Price, and J. Pullin, Phys. Rev. D (to be published), gr-qc/9802063
  - [4] J. Bowen and J. W. York, Jr., Phys. Rev. D 21, 2047 (1980).
  - [5] J. Baker and R. S. Puzio, preprint gr-qc/9802006.
  - [6] W. K. Rivlin and R. H. Price, Phys. Rev. D 58, 104003 (1998).
  - [7] S. R. Brandt and E. Seidel, Phys. Rev. D 52, 852 (1995); Phys. Rev. D 52, 870 (1995); Phys. Rev. D 54, 1403 (1995).
  - [8] R. H. Boyer and R. W. Lindquist, J. Math. Phys. 8, 265 (1967).
  - [9] S. A. Teukolsky, Astrophys. J. 185, 635 (1973).
  - [10] F. Zerilli, Phys. Rev. Lett. 24, 737, (1971).
  - [11] T. Regge and J. A. Wheeler, Phys. Rev. 108, 1063 (1957).
  - [12] In the Teukolsky formalism of Ref. [9] it is possible to separate the angular dependence of perturbations if perturbation functions are first decomposed into single frequency components. Such separation is useful for some

purposes, but not for the evolution of initial data, the problem in which we are interested.

- [13] W. K. Rivan, P. Laguna, P. Papadopoulos, and N. Andersson, Phys. Rev. D 56, 3395 (1997).
- [14] E. T. Newman and R. Penrose, J. Math. Phys. 3, 566 (1962).
- [15] C. W. Misner, K. S. Thorne and J. A. Wheeler, Gravitation (Freeman, San Francisco, 1973), Sec. 21.5.
- [16] M. Campanelli, W. K. Rivan, C. O. Lousto, Phys. Rev. D 58, 024016 (1998).
- [17] M. Campanelli, C. O. Lousto, J. Baker, G. Khanna, and J. Pullin, Phys. Rev. D 58, 084019 (1998).
- [18] S. Chandrasekhar, The mathematical theory of black holes (Oxford University Press, Oxford, 1983).
- [19] Edward W. Leaver, Ph.D. thesis, University of Utah, 1985.
- [20] A. M. Abraham, R. H. Price, Phys. Rev. D 53, 1972 (1996).

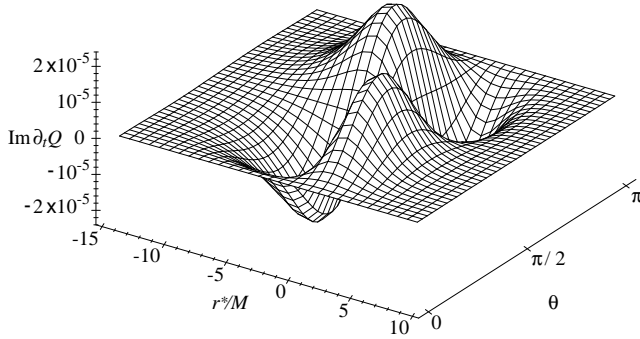


FIG. 1. Initial data for  $\text{Im } Q_t$  as a function of the spatial coordinates  $r$  and  $\theta$ . Note the antisymmetry with respect to the equatorial plane, given by  $\theta = \pi/2$ .

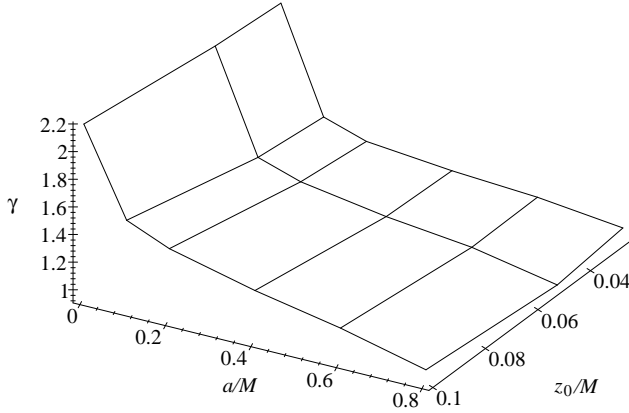


FIG. 2. The relative deviation  $\gamma = (K_{\text{err}} - K_{\text{true}})/K_{\text{true}}$  is evaluated at  $r = 0.5$ ,  $\theta = 0$ . For a given value of  $z_0$  we compute the relative deviation  $\gamma_{z_0}$  at  $z_0$ , and the relative deviation  $\gamma_{2z_0}$  at  $2z_0$ . The exponent is defined by  $\gamma_{2z_0} = 2^\alpha \gamma_{z_0}$ , so that  $\alpha$  is roughly an exponent in the relationship  $\gamma / \gamma_{z_0}$ . The figure shows that the dependence varies from approximately quadratic for small  $a$  to approximately linear for large  $a$ .

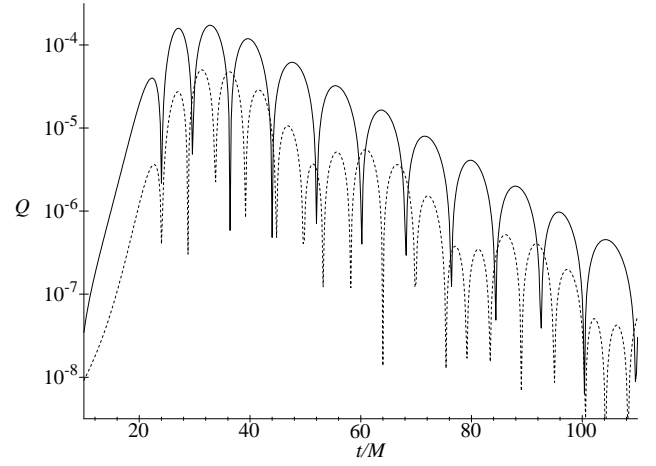


FIG. 3. Logarithmic representation of the radiation waveform  $\text{Re } Q$  (solid curve) and  $\text{Im } Q$  (dashed curve) as a function of  $t/M$  at  $r/M = 25$ ,  $\theta = 4$ , for a collision with  $a/M = 0.5$ , and  $z_0/M = 0.05$ . See text for discussion.

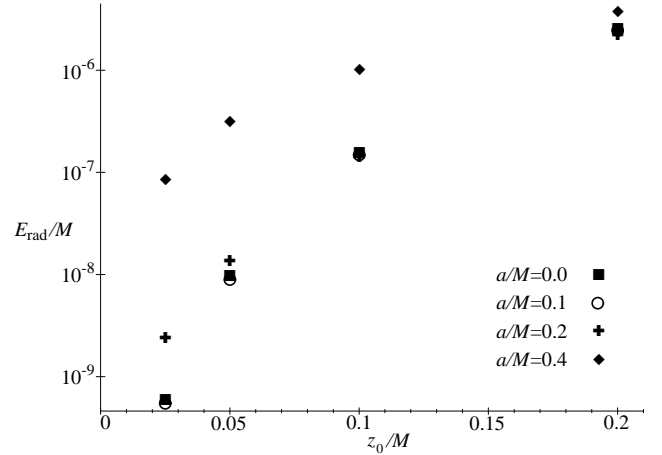


FIG. 4. The calculated total energy  $E_{\text{rad}}$  radiated in gravitational waves, as a function of  $z_0/M$  for different values of  $a$ . A meaningful demonstration of the influence of  $a$  would require a physical measure of separation in place of  $z_0$ . See text for details.